Airglow retrievals from the O_2 singlet delta band with MethaneAIR measured spectra and MethaneSAT synthetic spectra

Sébastien Roche[1,2,3], Christopher Chan Miller[1,3], Amir Souri[5,6], Jonas Wilzewski[2,3,*], Jenna Samra[3], Maryann Sargent[2], Bingkun Luo[3], Jonathan Franklin[2], Kang Sun[4], Kelly Chance[3], Xiong Liu[3], and Steven Wofsy[2]

1: Environmental Defense Fund, Washington, D.C., USA
2: Harvard John A. Paulson School of Engineering and Applied Sciences, Harvard University, Cambridge, MA, USA
3: Center for Astrophysics | Harvard & Smithsonian, Cambridge, MA, USA
4: Research and Education in Energy, Environment and Water Institute, University at Buffalo, Buffalo, NY, USA
5: Atmospheric Chemistry and Dynamics Laboratory, NASA Goddard Space Flight Center, Greenbelt, MD, USA
6: GESTAR II, Morgan State University, Baltimore, MD,USA
* Now at: EUMETSAT, Eumetsat Allee 1, 64295 Darmstadt, Germany

Contact: sroche@g.harvard.edu

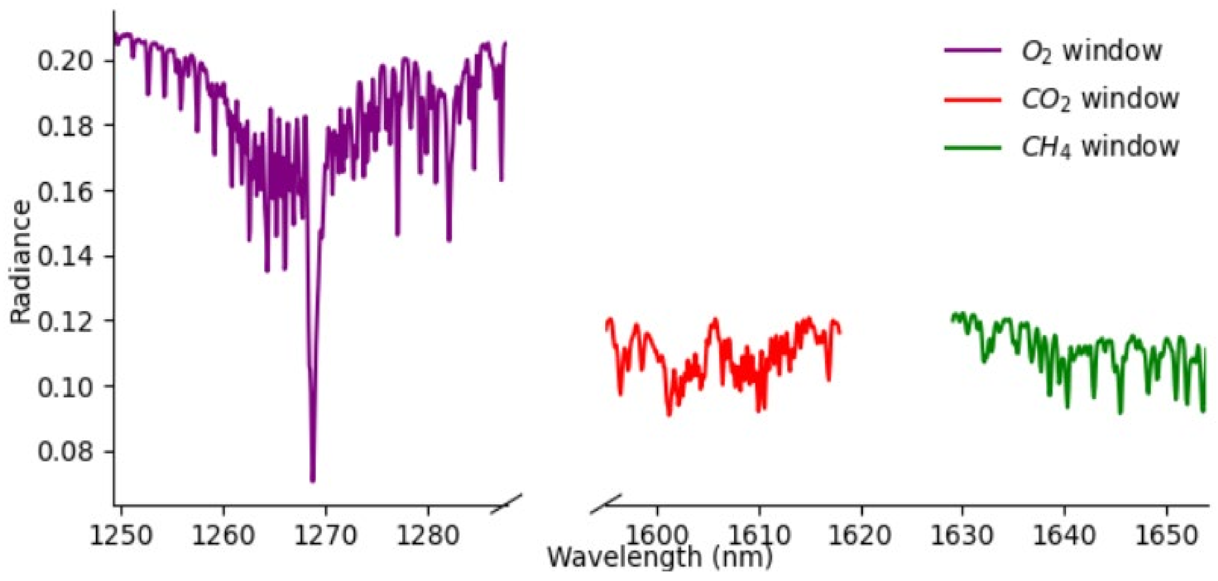

Figure 1: Example MethaneAIR spectrum from each spectral window.

The area-mapping MethaneSAT satellite (launched March 4, 2024) will aim to estimate CH_4 emissions from over 80% of oil & gas production. It uses one spectrometer to retrieve CH_4 from a window centered at 1.66 µm, and CO_2 from a window centered at 1.61 µm, and a second spectrometer to retrieve O_2 and surface pressure in a window centered at 1.27 µm (see Figure 1). MethaneAIR is the airborne simulator for the MethaneSAT satellite, its observations are used to test the retrieval algorithms that will be used to process MethaneSAT spectra, but also to obtain emissions estimates from oil & gas basins in the United States.

Operational retrievals for MethaneSAT will use "proxy" retrievals instead of "full physics" retrievals. A "proxy" retrieval does not include the effect of aerosols on the light path in the forward model, it instead uses the column of another gas retrieved from a band spectrally close to the target gas as proxy for the aerosol-induced light path changes, assuming that they are similar in the two neighboring spectral regions. Typically, CO_2 has been used as the proxy species for XCH_4, but the errors in the a priori XCO_2 can introduce biases, especially over targets with sources of both CH_4 and CO_2. XO_2 (~0.2095) is much less variable than XCO_2. However, the O_2 window is more spectrally distant from the CH_4 window than the CO_2 window, making the O_2 proxy more sensitive to aerosols. For MethaneSAT, the O_2 window will also be affected by airglow.

$$XCH_4^{CO_2-proxy} = XCO_2^{apriori}\frac{column_{CH_4}}{column_{CO_2}} \quad ; \quad XCH_4^{O_2-proxy} = XO_2^{apriori}\frac{column_{CH_4}}{column_{O_2}}$$

MethaneAIR first campaign took measurements over 10 research flights between 2019 and 2021. A second campaign of measurements occurred in Fall 2022, MethaneAIR-Extended (MethaneAIR-E), with 4 research flights. The third flight campaign happened in summer 2023 with 64 flights (MethaneAIR-X). The MethaneAIR instrument specifications are shown in Table 1. The aircraft typically flies at ~12-14 km altitude and observed spectra are thus unaffected by the airglow emission from excited oxygen molecules between ~ 25-75 km. During the last MethaneAIR flight (RF10, flight path in Figure 3) the spectrometer was looking upwards to record oxygen airglow emission spectra.

The MethaneAIR sensor has 1280 spatial pixels, but only 860 are illuminated. In the results presented here we used spectra aggregated in the spatial dimension by a factor 5, leading to 172 across-track pixels, there is no aggregation in the along-track dimension.

We performed full physics retrievals on RF10 spectra to obtain airglow columns. The oxygen fitting window is 38.6 nm wide from 1249.2 to 1287.8 nm. Some RF10 example measured spectra are shown in Figure 4, retrieval results from the full flight are shown in Figures 3 and 5.

We also performed a sensitivity experiment with a synthetic MethaneSAT pixel under a range of viewing geometries and surface albedo, but without including the effect of aerosol. The synthetic spectra are generated with airglow but fitted without including airglow in the forward model to estimate the maximum retrieval error that can be caused by airglow. Each observation condition is processed with 100 noise realizations.

In the forward model the airglow spectra are computed following Sun et al. (2018) Equations (4) and (5). The GGG2020 linelists (Toon and Mendonca, 2022) were used to derive absorption cross section lookup tables and the airglow emission rate lookup table.

A priori Airglow Profiles

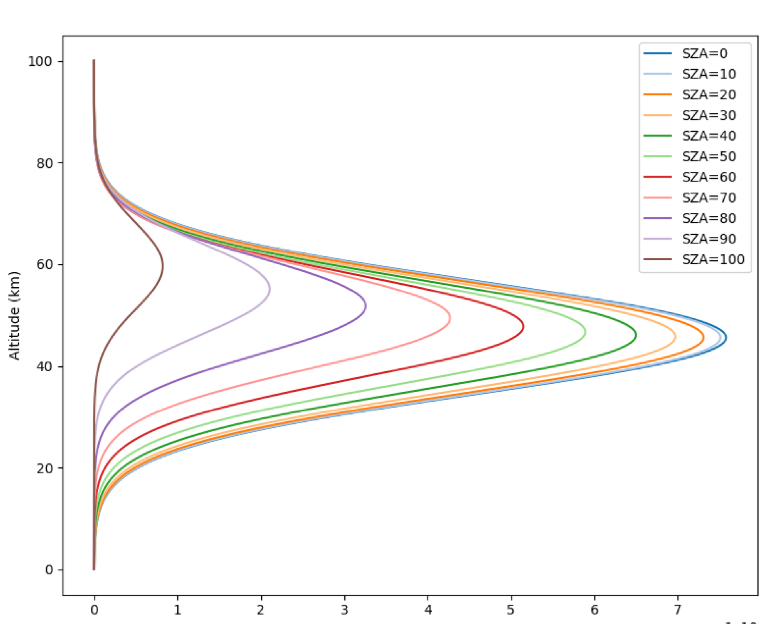

Figure 6 : density profiles of excited Oxygen (airglow) molecules obtained from a parametrization of SCIAMACHY measured profiles with solar zenith angle (code available on github: https://github.com/rocheseb/oxygen_airglow_lut).

To generate a priori airglow profiles, we derived a parametrization using airglow profiles measured by SCIAMACHY in 2010 (Sun et al., 2022).

The measured profiles were averaged in solar zenith angle (SZA) bins and were fitted with gaussian profiles in each bin. Then a SZA parametrization was derived for the gaussian mean (peak altitude), standard deviation, and intensity. The resulting parametrized profiles are shown in Figure 6.

Based on retrievals with MethaneAIR up-looking measurements these profiles systematically overestimate the airglow total column and are thus scaled by an empirical factor 0.6. The simple parametrization does not account for the Ozone column that the airglow density depend on. However, with the empirical scaling the retrieved scale factors are close to 1 at all SZAs.

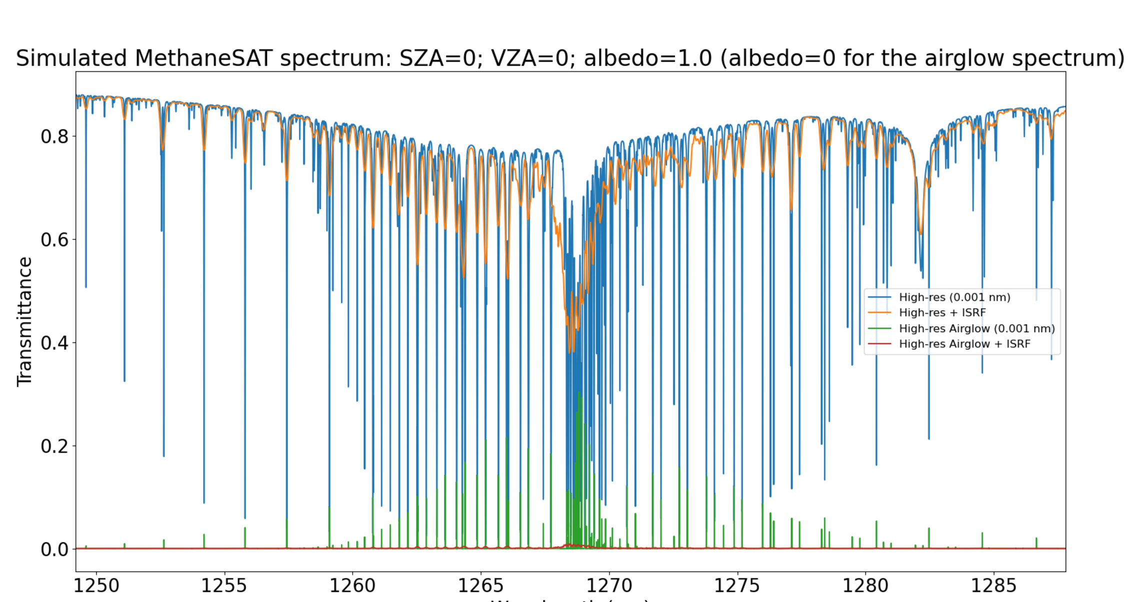

Figure 7: spectrum simulated with 0.001 nm spacing (blue); simulated spectrum with MethaneSAT instrument spectral response function applied (orange); airglow spectrum simulated with 0.001 nm spacing (green); simulated airglow spectrum with MethaneSAT ISRF applied (red).

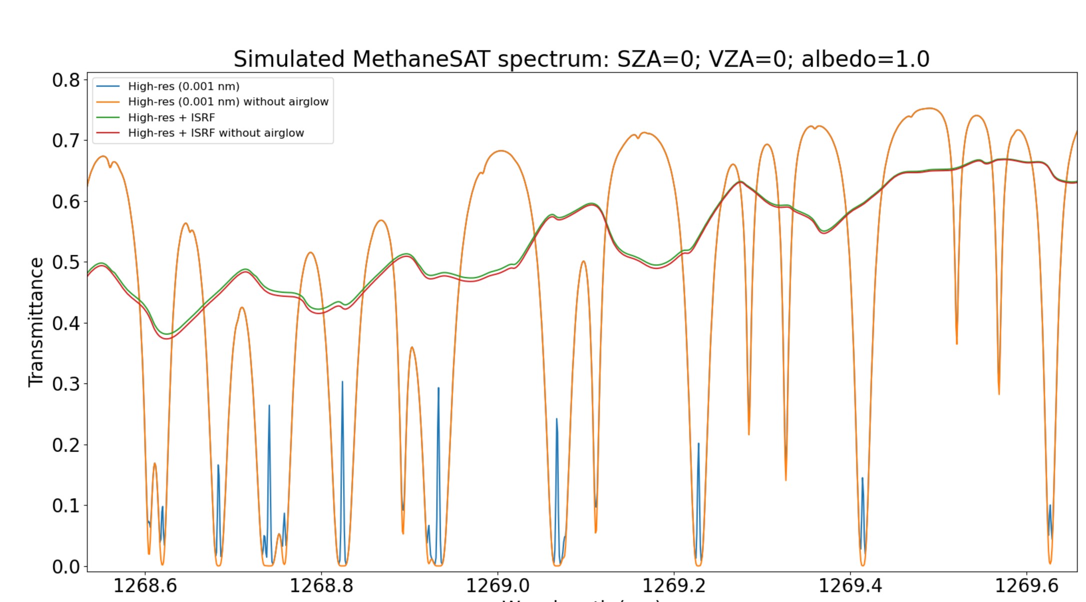

Figure 8: zoom on a subset of lines from a spectrum simulated with 0.001 nm spacing (blue); same but without including airglow (orange); simulated spectrum with MethaneSAT ISRF applied (green); same but without including airglow (red). With high resolution spectra we can see that airglow "dents" the O_2 absorption lines. But with the coarser spectral resolution of the instrument this results in a small and broad reduction in the signal.

Preliminary Results

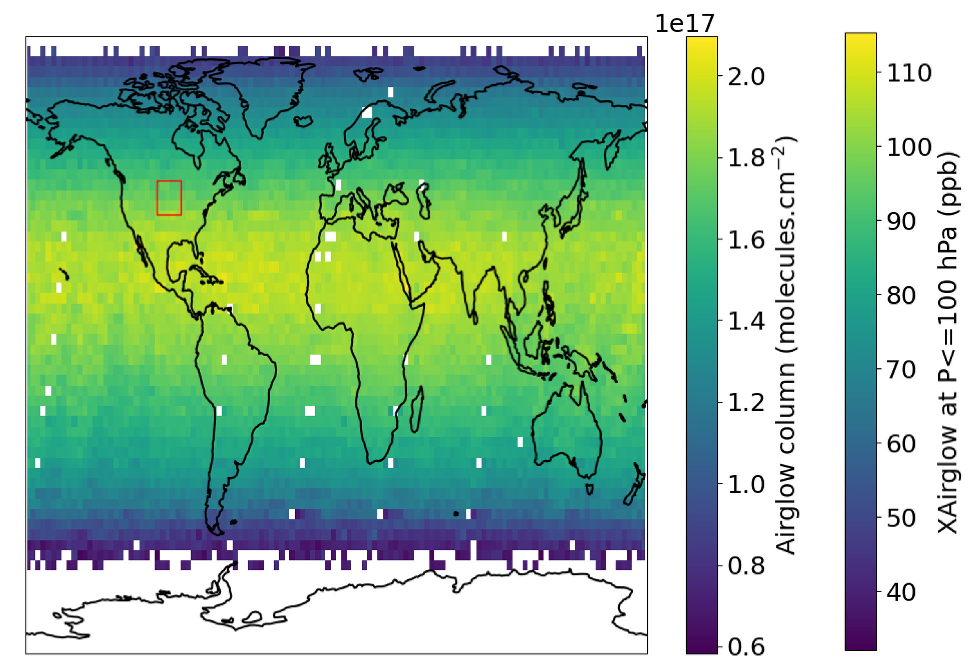

Figure 2: Airglow climatology from Sun et al. (2022) for the month of August, derived as the average of retrievals from all SCIAMACHY limb observations in August 2010. The color bars indicate the total column of airglow (left) and the column-averaged dry-air mole fraction of airglow (XAirglow) at pressures less than 100 hPa (right). The red rectangle marks the region where RF10 flew.

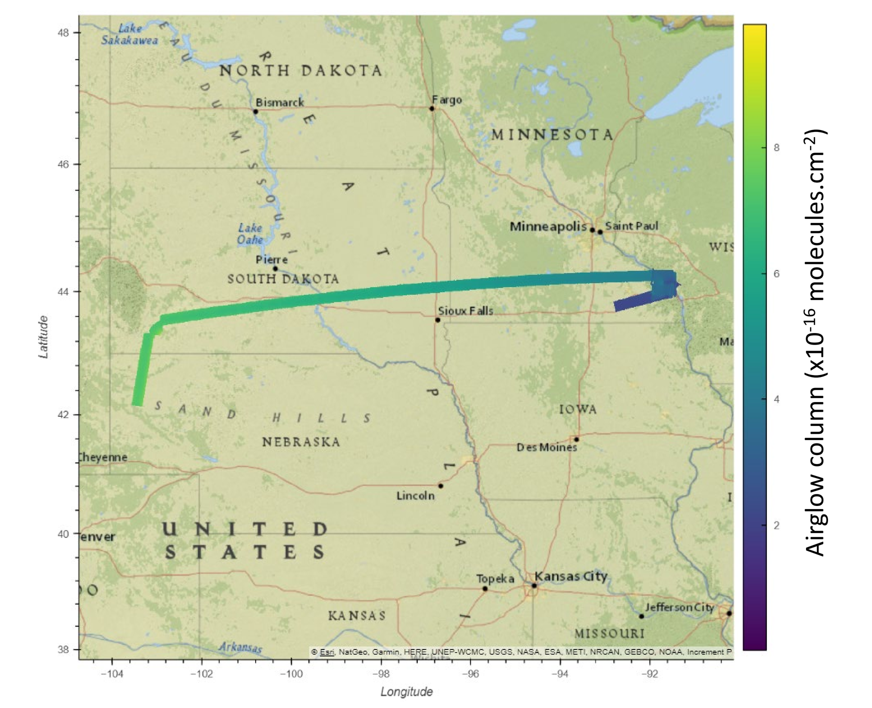

Figure 3: MethaneAIR RF10 retrieved total column of airglow.

Table 1: Specification comparison for MethaneAIR and MethaneSAT

Specification	MethaneAIR	MethaneSAT
O_2 passband (nm)	1237–1319	1249–1305
O_2 dispersion (nm/pixel)	0.08	0.06
O_2 spectral FWHM (nm)	0.23	0.18
CH_4 passband (nm)	1592–1678*	1598–1683
CH_4 dispersion (nm/pixel)	0.10	0.08
CH_4 spectral FWHM (nm)	0.28	0.24
Field of view (°)	23.7	21.3
Cross-track pixel† (m)	~ 5 at 12 km	~ 108
Along-track pixel† (m)	~ 25	~ 400
Point spread function (pixels)	2.5	1.8
single pixel SNR‡	~ 110	~ 190

*MethaneAIR uses an InGaAs detector with reduced QE beyond ~ 1660 nm
†Distance between pixel centers at nadir
‡CH_4 band with nominal radiance of 1.4×10^{13} photons cm^{-2} nm^{-1} sec^{-1} sr^{-1}

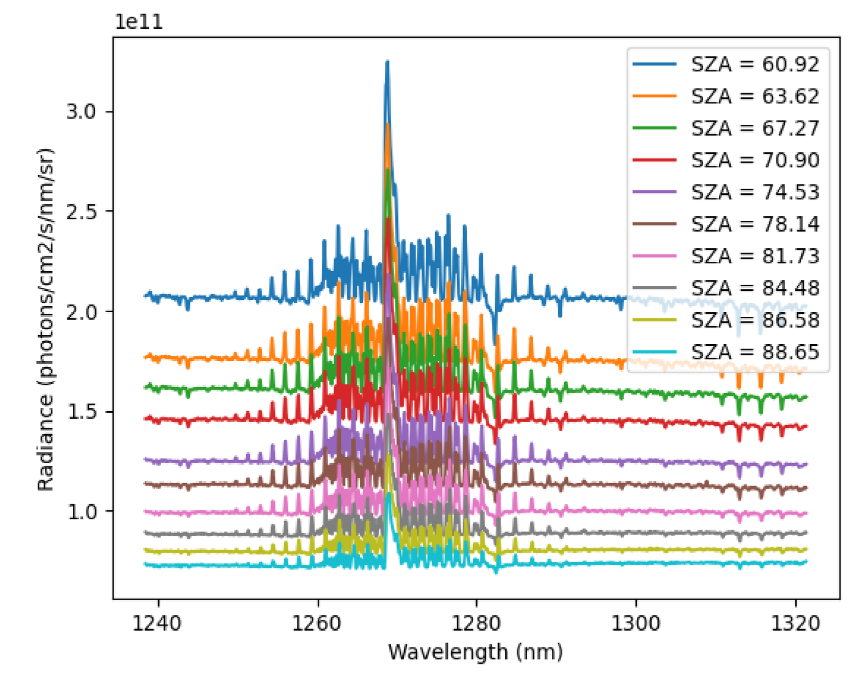

Figure 4: MethaneAIR RF10 measured spectra, each spectrum is the average from 172x61 pixels (across-track x along-track).

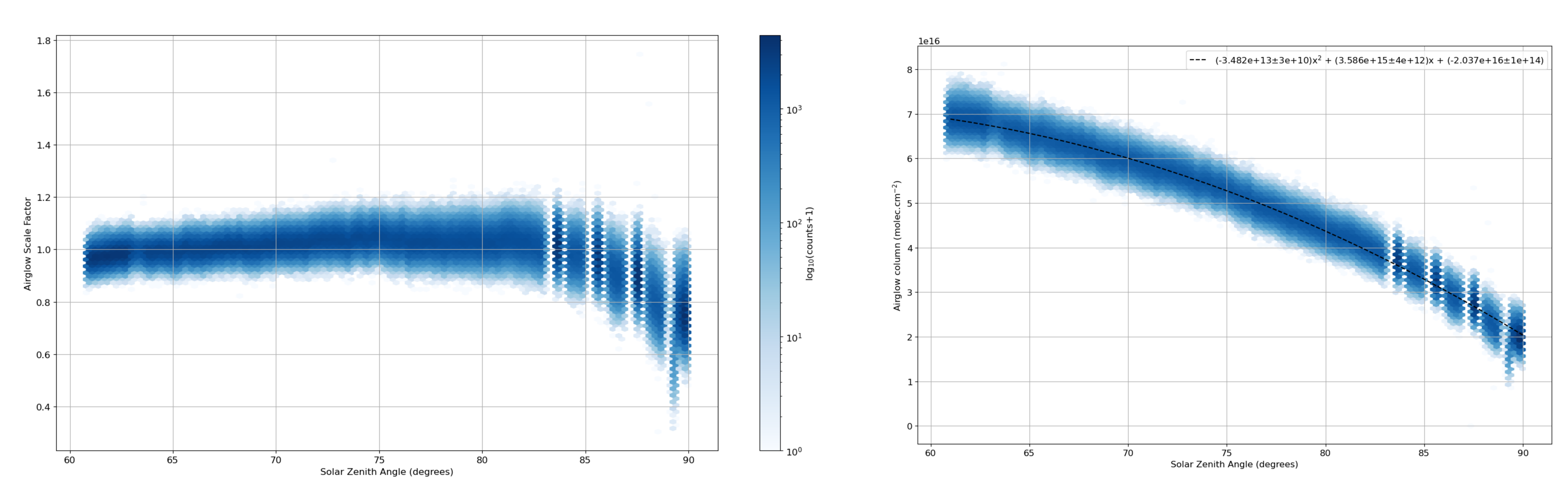

Figure 5: retrieved scale factor (left) and retrieved total column of airglow (right) vs solar zenith angle. A quadratic fit to the airglow column is also shown.

Preliminary results indicate little spatial variability in airglow over the MethaneAIR RF10 flight path.
After removing the SZA dependence, the standard deviation of the airglow column is ~2.2e15 molecules.cm^{-2} (~3-11% between ~60-90 SZA).

Simulated MethaneSAT O_2 spectra

Synthetic MethaneSAT spectra were simulated over a range of SZA, viewing zenith angles (VZA), and surface albedos. Figures 7 and 8 show an example synthetic spectrum before and after applying the MethaneSAT instrument spectral response function (ISRF).

The MethaneSAT noise model was applied to produce 100 realizations of each observation conditions. These synthetic spectra were then fitted without including airglow in the forward model.

Results show that under the best conditions (low airmass and high albedo) the error on the retrieved surface pressure is ~2% (Figure 9). This would lead to a ~30-40 ppb minimum bias in $XCH_4^{O_2-proxy}$.

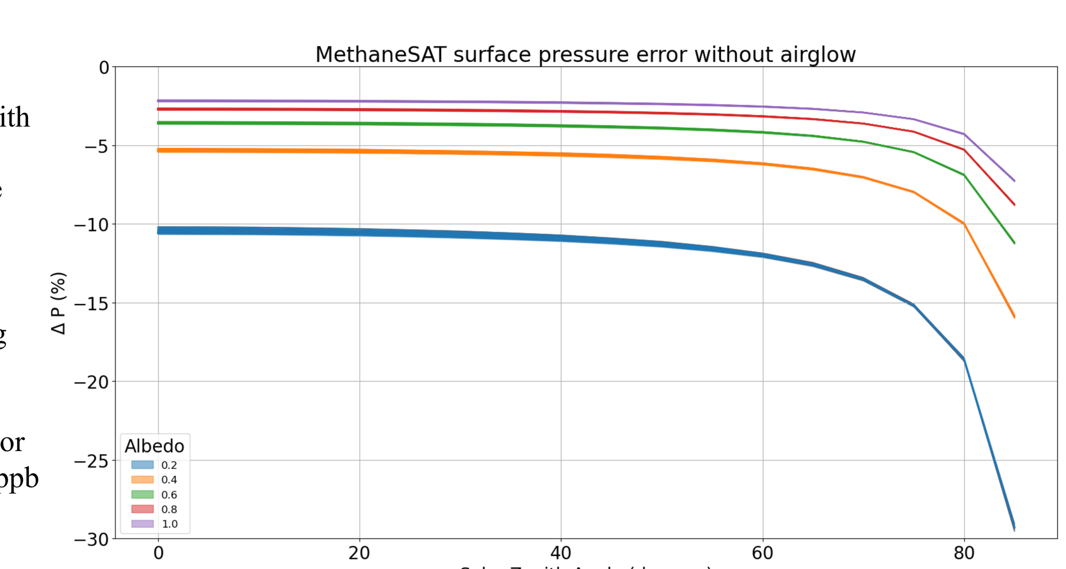

Figure 9: surface pressure error caused by not including airglow in the forward model. Includes 855 simulations with SZA from 0-85, VZA from 0-40, and surface albedo from 0.2-1. At each albedo, the bands encompass 8 lines with the different VZAs.

References

Staebell, C., Sun, K., Samra, J., Franklin, J., Chan Miller, C., Liu, X., Conway, E., Chance, K., Milligan, S., and Wofsy, S.: Spectral calibration of the MethaneAIR instrument, Atmos. Meas. Tech., 14, 3737–3753, https://doi.org/10.5194/amt-14-3737-2021, 2021.

Sun, K., Gordon, I. E., Sioris, C. E., Liu, X., Chance, K., & Wofsy, S. C. (2018). Reevaluating the use of O_2 $a^1\Delta_g$ band in spaceborne remote sensing of greenhouse gases. *Geophysical Research Letters*, 45, 5779– 5787. https://doi.org/10.1029/2018GL077823

Sun, K., Yousefi, M., Chan Miller, C., Chance, K., González Abad, G., Gordon, I. E., Liu, X., O'Sullivan, E., Sioris, C. E., and Wofsy, S. C.: An optimal estimation-based retrieval of upper atmospheric oxygen airglow and temperature from SCIAMACHY limb observations, Atmos. Meas. Tech., 15, 3721–3745, https://doi.org/10.5194/amt-15-3721-2022, 2022.

Sun, Kang, 2022, "Level 2 data for SCIAMACHY airglow retrieval in 2010", https://doi.org/10.7910/DVN/T1WRWQ, Harvard Dataverse, V1

Toon, G. C. (2022). Atmospheric Non-Voigt Line List for the TCCON 2020 Data Release (GGG2020.R0) [Data set]. CaltechDATA. https://doi.org/10.14291/TCCON.GGG2020.ATMNV.R0